En Face Enhanced Depth Imaging Optical Coherence Tomography of Fibrovascular Pigment Epithelium Detachment

Florence Coscas,[1,2,4] *Gabriel Coscas,*[1,2] *Giuseppe Querques,*[1,3,4] *Nathalie Massamba,*[1] *Lea Querques,*[3] *Francesco Bandello,*[3] *and Eric H. Souied*[1]

Purpose. To analyze the internal structure of fibrovascular pigment epithelial detachment (FV-PED) due to AMD using en face enhanced depth imaging (EDI) spectral-domain optical coherence tomography (SD-OCT).

Methods. Thirty-eight consecutive patients presenting with FV-PED due to AMD were enrolled in this study. Retinal images were automatically obtained with a spectral domain (SD) OCT instrument; the typical inverted 97 sections at 30-μm intervals, each comprised of nine averaged B-scans, were acquired in less than 60 seconds. The resultant images of en face cross-sections of the choroid (C-scans) were compared with indocyanine green angiography (ICGA) images, currently the only technique available for directly viewing occult choroidal neovascularization (CNV).

Results. Thirty-eight eyes of 38 consecutive patients (27 females and 11 males, mean age 76.7 ± 3 years) were studied. In all 38 eyes, ICGA allowed visualization of the CNV within the FV-PED. In 30 eyes, en face EDI-OCT revealed what appeared to be the hyperreflective course of presumed CNV, which was located just beneath the detached retinal pigment epithelium; this was confirmed by comparative analysis of the extent of hyperreflective lesions on en face EDI-OCT images and that of the neovascular network on ICGA. An area of homogeneous hyporeflectivity, consistent with serous exudation, separated the CNV from the Bruch's membrane and the choroid. In the remaining eight eyes, en face EDI-OCT revealed homogenous hyperreflectivity, consistent with fibrous tissue that partially hid the neovascular network.

Conclusions. Noninvasive en face EDI-OCT technique enables visualization and localization of the entire branching neovascular network of CNV within FV-PED without dye injection. (*Invest Ophthalmol Vis Sci.* 2012;53:4147–4151) DOI: 10.1167/iovs.12-9878

From the [1]Department of Ophthalmology, University Paris Est Creteil, Centre Hospitalier Intercommunal de Creteil, Creteil, France; the [2]Centre d'Ophtalmologie de l'Odeon, Paris, France; and the [3]Department of Ophthalmology, University Scientific Institute San Raffaele, Milan, Italy.

[4]These authors contributed equally to the work presented here and should therefore be regarded as equivalent authors.

Submitted for publication March 19, 2012; revised May 20, 2012; accepted May 21, 2012.

Disclosure: **F. Coscas**, None; **G. Coscas**, Allergan, Novartis, Optovue (C, R); **G. Querques**, None; **N. Massamba**, None; **L. Querques**, None; **F. Bandello**, Alcon, Alimera, Allergan, Bayer, Bausch & Lomb, Farmila-Thea, Genentech, Novartis, Pfizer (C, R); **E.H. Souied**, Alcon, Bausch & Lomb, Chauvin, Novartis (C, R)

Corresponding author: Gabriel Coscas, Department of Ophthalmology, University Paris-Est Creteil, Centre Hospitalier Intercommunal de Creteil, 40 Avenue de Verdun, 94000 Creteil, France; gabriel.coscas@gmail.com.

Exudative AMD is characterized by abnormal growth of newly formed blood vessels, known as choroidal neovascularization (CNV). By analyzing enucleated eyes, Gass classified the neovascular growth pattern as RPE (type 1); subretinal (type 2); or combined.[1] Gass hypothesized that in type 1 CNV, exudation from neovascularization spread laterally detaching the surrounding RPE monolayer by hydrostatic dissection above the level of the leaking vessels.[2] This hypothesis led to the term fibrovascular pigment epithelial detachment (FV-PED) to distinguish this form of exudative AMD from other forms of serous pigment epithelial detachment (PED).

Indocyanine green angiography (ICGA) was introduced in the 1970s for imaging the choroidal circulation because of the particular optical properties of this dye.[3] ICG absorbs and reflects in the near-infrared portion of the spectrum (805 nm and 835 nm, respectively), and thus renders the RPE invisible. Yannuzzi and associates[4] demonstrated that ICGA allows visualization of the entire choroidal neovascular membrane in type 1 CNV.

Recently, a new technique to improve depth imaging by optical coherence tomography (OCT), termed enhanced depth imaging (EDI)-OCT, has been shown to reliably image the full-thickness of the choroid.[5] The EDI-OCT technique uses a spectral domain (SD)-OCT instrument (Spectralis SD-HRA-OCT; Heidelberg Engineering, Heidelberg, Germany), which is positioned closer to the eye than has been usual, producing a stable inverted image. The net effect of this technique is increased sensitivity of the imaging in deeper layers of tissue. Using a time domain OCT instrument, study authors showed a layer of tissue behind the RPE in PED associated with type 1 CNV.[6] Using the B-scan EDI-OCT technique to investigate the internal structure of FV-PED, Spaide showed moderately hyperreflective material on the back surface of the RPE that could be suggestive of presumed CNV.[7]

A new approach to OCT imaging, called "en face OCT," combines SD-OCT with transverse confocal analysis.[8] The en face OCT technique produces simultaneous longitudinal (B-scans) and transverse (C-scans) images of the macular area with high pixel-to-pixel correspondence. Based on available data, en face cross-sections of the choroid (C-scans) reconstructed from EDI-OCT B-scans, have not yet been used for the evaluation of choroidal and sub-RPE changes in FV-PED.

In this study, authors reported a method they developed to visualize and localize the neovascular network in the internal structure of FV-PED due to AMD using the en face EDI-OCT technique. This analysis may offer a clearer picture of the neovascular process and provide insights into the pathophysiology of FV-PED development.

Methods

Study authors enrolled 38 consecutive patients with FV-PED due to exudative AMD who presented at the University Eye Clinic of Creteil, at

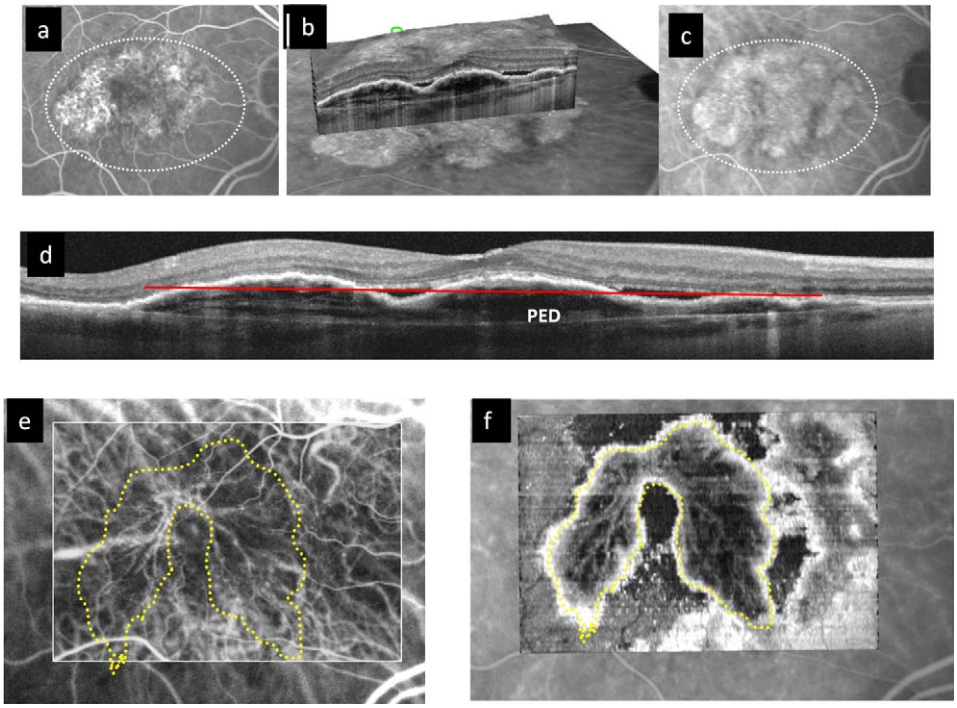

Figure 1. Multimodal imaging of FV-PED in a treatment-naïve eye with AMD. (**a**) FA (*top left panel*) shows heterogeneous speckled hyperfluorescence of a large irregular plurilobular FV-PED (*white circle*). (**b**) OCT volume (*top middle panel*) superimposed on ICGA image, with B-scan horizontal, anterior-posterior section, in EDI-OCT. (**c**) ICGA late phase (*top right panel*) shows visualization of the entire choroidal neovascular membrane (*white circle*) in the area occupied by FV-PED. (**d**) Horizontal EDI-OCT B-scan (*middle panel*) shows presence of linear hyperreflective lesions within the dark FV-PED, suggestive of the hyperreflective course of the type 1 CNV. The *red line* represents the section plane of (**f**). (**e**) Enlarged early phase ICGA (*bottom left panel*) shows visualization of the entire choroidal neovascular membrane (*yellow dotted line*) in the area occupied by FV-PED. (**f**) Same size view of en face EDI-OCT (*bottom right panel*) shows the hyperreflective internal structure of FV-PED, which is consistent with the hyperreflective course of the type 1 CNV. The network is clearly visible in the upper part of the cavity of FV-PED, lying just beneath the surface of the detached RPE. A limited amount of subretinal fluid (SRF) accumulation is detectable, surrounding the elevated FV-PED.

Centre d'Opthalmologie de l'Odeon, and at the University Eye Clinic of San Raffaele Hospital, between October and December 2011. To be included for analysis, patients with FV-PED had to undergo, as part of their routine clinical work-up, ICGA and EDI-OCT over a $15° \times 10°$ area to encompass the FV-PED. Exclusion criteria were poor quality images due to extreme eye movement or extensive media opacities; diagnosis of drusenoid or avascular PED; presence of serous PED due to causes other than AMD; and signs of any other active retinal disease in the study eye such as retinal vascular (i.e., diabetic retinopathy and retinal vein occlusion) or vitreoretinal diseases (i.e., vitreomacular traction syndrome and epiretinal membrane).

The study followed the tenets of the Declaration of Helsinki. Written informed consent was obtained from the patients after explanation of the nature and possible consequences of the study. Approval for this study was obtained from the Ethics Committee of the San Raffaele Hospital, Milan, Italy.

Study Protocol

Best-corrected visual acuity (BCVA) was determined in all subjects using the Early Treatment Diabetic Retinopathy Study (ETDRS) charts. Retinal status was evaluated by fundus biomicroscopy by three experienced retinal physicians (FC, GQ, and GC) after pupil dilation, fluorescein angiography (FA), and ICGA. Automated central macular thickness (CMT) measurements were generated by a spectral domain (SD)-OCT instrument (Heidelberg Engineering) using a 19-horizontal line protocol (6×6-mm area), each consisting of 1024 A-scans per line (Spectralis Acquisition and Viewing Modules, version 5.3.2; Heidelberg Engineering). All subjects underwent choroidal imaging by ICGA and EDI-OCT.

ICGA and En Face EDI-OCT Analysis

A standardized imaging protocol was performed on all patients, which included acquisition of early, mean, and late phase ICGA frames (excitation $\lambda = 787$ nm; emission $\lambda > 800$ nm; field of view, $30° \times 30°$; image resolution, 768×768 pixels). With confocal image acquisition, light from a conjugate plane of interest is detected by the image sensor, permitting suppression of light from planes anterior and posterior to the plane of interest, resulting in high-contrast fundus images. Using automated eye tracking and image alignment based on cSLO images, the software allows averaging a variable number of single images in real time (ART [Automatic Real Time] Module; Heidelberg Engineering).

For each study eye, one early/mean ICGA ART image (up to 100 single images) showing the extent of neovascular network was selected by three authors (FC, LQ, and NM) for further analysis.

The method of obtaining EDI OCT images has been reported previously.[5] The choroid was imaged by positioning the SD-OCT close enough to the eye to obtain an inverted image. Ninety-seven sections, each comprised of nine averaged EDI OCT B-scans at 30-μm intervals, were automatically obtained within a $15° \times 10°$ rectangle to encompass the FV-PED; this acquisition was automatic and completed in approximately 60 seconds. The resultant 496 en face images from the vitreous cavity and inner retinal surface up to the outer sclera were viewed with the incorporated software platform (Heidelberg Eye Explorer, version 1.7.0.0; Heidelberg Engineering). The FV-PED was evaluated by three authors (FC, GQ, and GC) to ascertain the presence, location, and extent of hyperreflective lesions. Study authors classified the variability in reflectivity, including hyperreflectivity, as described by Hee et al. in 1996.[9] The most meaningful en face EDI-OCT images were analyzed on frozen images by scrolling the mouse button. Retinal vessel crossing points were automatically used as constant landmarks

to allow alignment of the en face EDI-OCT images with that of the ICGA images. Each layer was switched on and off to evaluate correspondence between the extent of hyperreflective lesions on en face EDI-OCT and that of the neovascular network on ICGA. Analysis was performed by three observers (FC, GC, and GQ).

Statistical Analysis

Statistical calculations were performed using survey authoring and deployment software (Statistical Package for Social Sciences [SPSS], version 17.0; SPSS Inc., Chicago, IL). Intergroup comparisons of BCVA (converted to the logarithm of the minimum angle of resolution [LogMAR]) and CMT were performed using the Student's *t*-test. The chosen level of statistical significance was $P < 0.05$.

Results

Demographics and Clinical Data of the Study Population

Thirty-eight eyes of 38 consecutive patients (27 females and 11 males, mean age 76.7 ± 3 years) with type 1 CNV and FV-PED due to exudative AMD met the inclusion criteria and were included in the analysis. Twelve out of 38 eyes were treatment-naïve, while 17 out of 38 eyes had undergone previous intravitreal anti-VEGF injections. There was no significant difference in age between the treatment-naïve and treated patients. Treated patients received a mean of 9 ± 5.5 (range 3–20) intravitreal anti-VEGF injections over a mean of 13.6 ± 6.1 (range 3–30) months. Mean Log MAR BCVA was 0.27 ± 0.13 and 0.37 ± 0.19 in treatment-naïve and treated patients, respectively ($P = 0.3$). Mean CMT was 348.8 ± 87.2 and 303.6 ± 46.2 in treatment-naïve and treated patients, respectively ($P = 0.2$).

Combined ICGA and En Face EDI-OCT Imaging

In all 38 eyes, ICGA allowed visualization of the entire choroidal neovascular membrane in the area occupied by FV-PED (Figs. 1, 2). Evaluation of single EDI-OCT B-scans (97 sections per eye) showed the presence of hyperreflective lesions within the FV-PED (Figs. 1–3). Also, on single EDI-OCT B-scans, the full thickness of the choroid was visualized in all eyes. In 30 out of 38 eyes (Group 1), the hyperreflective lesions within the FV-PED were arranged in discrete collections and internal layers, with dense hyperreflective collections along the back surface of the PED (Figs. 1, 3). Hyporeflective regions within the FV-PED, with fluid accumulation, were seen beneath the hyperreflective collections.[9] The remaining eight eyes (Group 2) showed only dense homogeneous hyperreflective collections within the FV-PED, consistent with fibrous tissue without fluid accumulation (Fig. 4). No or only small hyporeflective regions were seen beneath the dense hyperreflective collections, followed by the normal choroid vessels.

In all 30 eyes from Group 1, analysis of en face EDI-OCT imaging revealed what appeared to be the hyperreflective course of type 1 CNV within the hyporeflective PED. The branching network with even small caliber vessels was clearly visible in the upper part of the cavity of FV-PED, lying just beneath the undersurface of the detached RPE (Figs. 1, 2). Within the cavity of the PED but deeper, there was a hyporeflective area, optically empty, suggestive of fluid accumulation, separating the CNV from the normal choroid. Finally, deeper and out of the PED, choroid vessels became clearly visible (Fig. 3). A limited amount of subretinal fluid accumulation was detectable surrounding the elevated FV-PED.

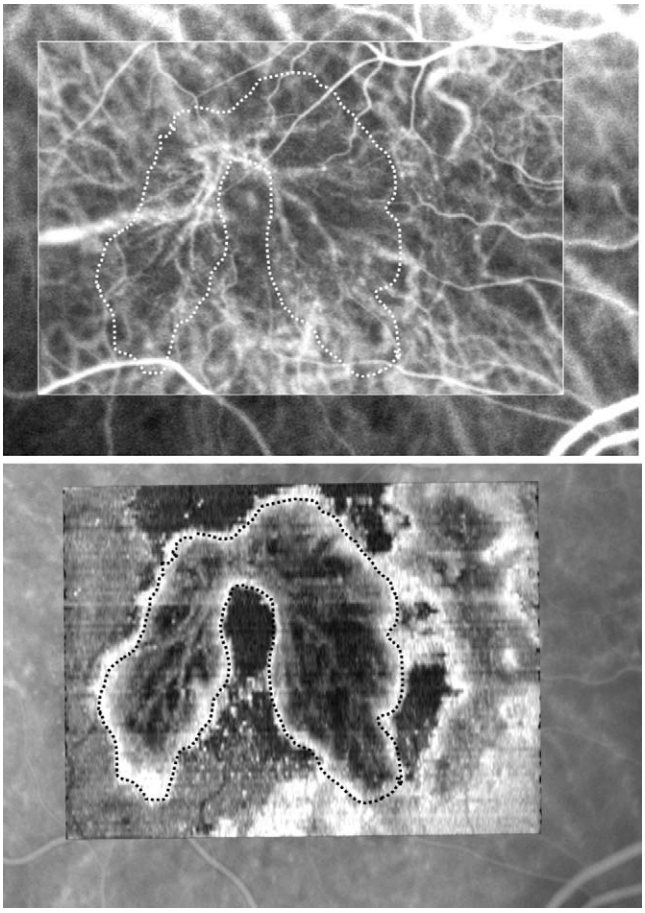

Figure 2. Comparison between ICGA (early phase) and en face OCT technique images, at similar magnification. The images show the exact coincidence of the course of the choroidal new vessels. (The limits of the PED are respectively indicated by the *dotted white* and *dotted black lines*.)

In all 30 eyes from Group 1, the hyperreflective course of type 1 CNV within the hyporeflective PED was confirmed by comparative analysis of the extent of hyperreflective lesions on en face EDI-OCT imaging and that of the neovascular network on ICGA. This observation was clearly demonstrated in Figure 2 and in supplemental Figures S1–S5 (see Supplementary Material, http://www.iovs.org/lookup/suppl/doi:10.1167/iovs.12-9878/-/DCSupplemental). Concordance between observers was very high (intraobserver, 97%; interobserver, 98%). Twelve out of these 30 eyes were treatment-naïve.

In all eight eyes with only dense homogeneous hyperreflective collections and without internal layers on EDI-OCT B-scans, analysis of en face EDI-OCT imaging revealed homogenous hyperreflectivity, consistent with fibrous tissue that hid the neovascular network (Fig. 4). In all eight eyes, the normal choroid vessels followed the homogenous hyperreflective lesion. All eight eyes had undergone previous multiple intravitreal anti-VEGF injections.

Discussion

FA, ICGA, and, increasingly, OCT are standard methods of examination in exudative AMD. FA visualizes the distribution of fluorescein molecules not only within vessels, but also in fluid-filled spaces, because fluorescein is only 80% protein bound; therefore, the free fluorescein readily escapes through the

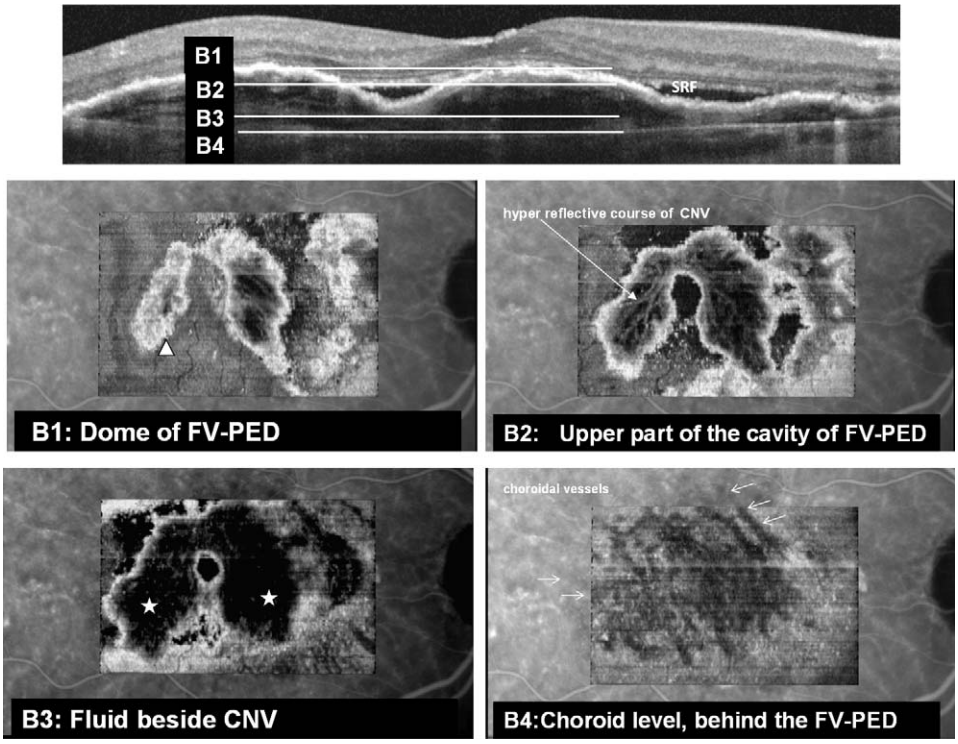

Figure 3. En face EDI SD-OCT imaging of FV-PED, at different levels of segmentation. Horizontal EDI-OCT B-scan (*top panel*). The *white lines* represent four different section planes imaged in B1, B2, B3, and B4. B1: At the dome of RPE elevation, the limits of the cavity become partially visible; retinal vessels are visible around the PED (*white arrow head*). B2: Inside the PED and immediately along the back surface of the RPE, hyperreflective course of type 1 CNV, contrasting with hyporeflective PED (*white arrow*). B3: Deeper in the cavity of the PED, serous fluid accumulation (*white star*). B4: Deeper and out of the PED, choroid vessels become clearly visible (*white arrows*).

fenestrations of the choriocapillaris and obscures the details of the underlying choroid. Conversely, because of the particular optical properties of the ICG dye,[3] which is highly bound to protein and does not readily escape from the choriocapillaris, ICGA allows a more detailed visualization of the entire CNV, especially in cases of type 1 CNV, which is not possible with FA.[4] However, both FA and ICGA are techniques that involve intravenous dye administration.

Non-invasive B-scan SD-OCT enables the imaging of the retinal structures, including visualizing the exudative reaction of the neovascular network in exudative AMD, by providing anterior-posterior sections. However, B-scan SD-OCT is compromised in terms of identifying sub-RPE CNV, since CNV is not directly visible but is only suggested by a sub-RPE area of hyperreflectivity[5] and by fluid accumulation (either sub-RPE, subretinal, or intraretinal). [6]

In this study, authors compared en face EDI-OCT images, obtained using the SD-OCT instrument, of the internal structure of FV-PED due to AMD with FA and also with ICGA images of type 1 CNV since ICGA allows conversion of the entire choroidal neovascular membrane of type 1 occult CNV into a well-defined network. The findings indicate that the extent of the hyperreflective course of what appeared to be CNV on en face EDI OCT images exactly corresponded with the hyperfluorescent neovascular network on ICGA images.

In this study, comparison between FA and ICGA were used to demonstrate the exact correspondence. In clinical routine, this technique of en face EDI-OCT may be easily used with monochromatic infrared images and without any injection of dye. Based on available data, this is the first demonstration that en face EDI-OCT technique enables detailed visualization of type 1 CNV in selected cases of FV-PED due to AMD. Thus, aspects that may render B-Scan SD-OCT inferior to angiography can be overcome by using the novel en face EDI-OCT technique.

This study's analysis also gives insight into the pathophysiology of FV-PED development. In a previous study, using time domain OCT, study authors showed a layer of tissue behind the RPE in PED associated with type 1 CNV.[6] Similar findings have been recently reported by Spaide using the B-scan EDI-OCT technique.[7] In this study, study authors showed that the hyperreflective course of type 1 CNV was closely in contact and lay just beneath the surface of the detached RPE, with a variable amount of homogeneous hyporeflectivity within the PED separating the CNV from the normal choroid. Given that the RPE secretes VEGF,[10,11] and that increased VEGF plays a fundamental role in the generation of CNV,[12,13] it is not surprising that the CNV may have an intimate association with the RPE. As the CNV spreads beneath the RPE, exudation from the CNV and fluid accumulation may develop exceeding the outflow ability of a relatively hydrophobic Bruch's membrane

For the first time, the presence and localization of CNV are shown and demonstrated in the PED. Until now, CNV were not detectable on SD-OCT but only suggested by a sub-RPE area of hyper reflectivity and by the fluid accumulation (either sub-RPE or sub and intraretinal).

There are several limitations to this study, primarily due to the absence of a control group (i.e., serous avascular PED) and lack of histopathologic confirmation of the visualized CNV. However, there was excellent correspondence between the "presumed" occult CNV seen using the en face EDI-OCT technique and the occult neovascular network seen on ICGA, currently the only technique available for directly viewing occult CNV.

In conclusion, study authors have shown for the first time that, in addition to the possibility of analyzing the contour and shape of a PED as reported for other en face OCT techniques,[14]

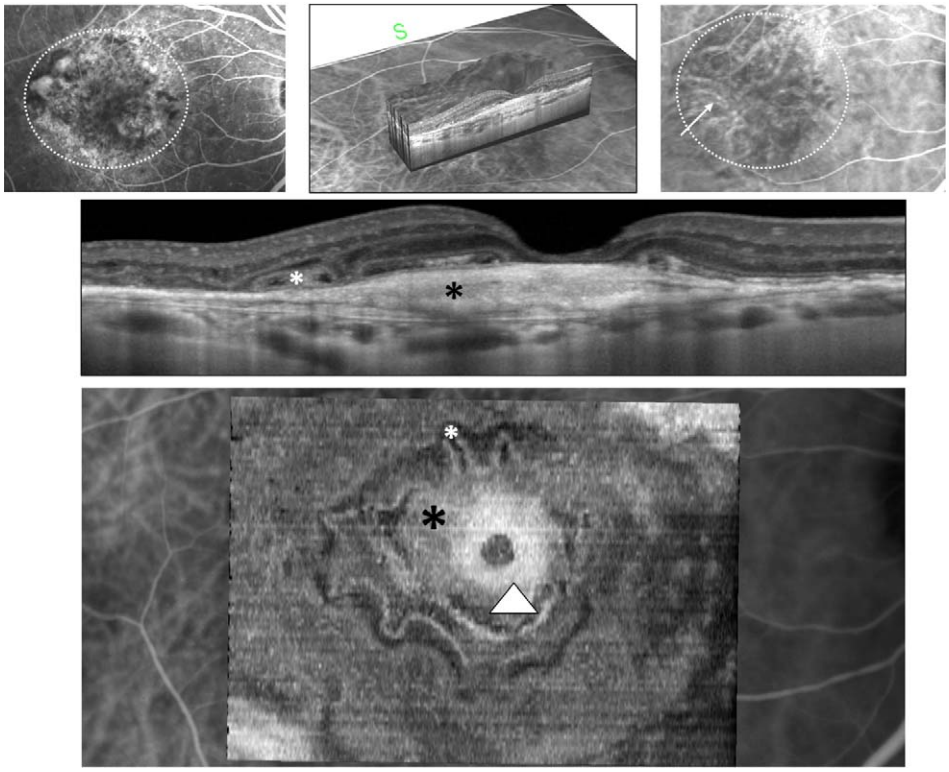

Figure 4. Multimodal imaging of FV-PED in an eye treated for AMD. FA (*top left panel*) shows moderate staining and limited leakage at the periphery of an extensive lesion with large irregular FV-PED (*white circle*). OCT volume (*top middle panel*) superimposed on ICGA image, with B-scan horizontal, anterior-posterior section, in EDI-OCT. ICGA (*top right panel*): the choroidal neovascular membrane (*white arrow*) is not distinctly visible in the area occupied by FV-PED (*white circle*). Horizontal EDI-OCT B-scan (*middle panel*) shows large homogenous hyperreflectivity (*black star*) within the FV-PED due to extensive fibrosis; there are degenerative changes and tubulations (*white star*) but no subretinal fluid. Enlarged view of en face EDI-OCT (*bottom panel*) shows the hyperreflective fibrosis (*white arrow head*), occupying most of the cavity of the fibrovascular PED (*black star*), and hiding the neovascular network; this is suggestive of extensive fibrosis. Note the irregular borders of the fibrovascular PED and tubulations (*white star*).

the en face EDI-OCT technique allows clear visualization and localization of the CNV within the FV-PED. This observation has clinical relevance since the en face OCT technique using an SD-OCT instrument is noninvasive and does not require a dye injection.

References

1. Gass JD. Biomicroscopic and histopathologic considerations regarding the feasibility of surgical excision of subfoveal neovascular membranes. *Am J Ophthalmol*. 1994;118:285–298.
2. Gass JD, Norton EW, Justice J Jr. Serous detachment of the retinal pigment epithelium. *Trans Am Acad Ophthalmol Otolaryngol*. 1966;70:990–1015.
3. Flower RW, Yannuzzi LA, Slakter JS. History of indocyanine green angiography. In: Yannuzzi LA, Flower RW, Slakter JS. *Indocyanine Green Angiography*. St Louis, MO: Mosby; 1997:2–17.
4. Yannuzzi LA, Slakter JS, Sorenson JA, Guyer DR, Orlock DA. Digital indocyanine green videoangiography and choroidal neovascularization. *Retina*. 1992;12:191–223.
5. Spaide RF, Koizumi H, Pozonni MC. Enhanced depth imaging spectral-domain optical coherence tomography. *Am J Ophthalmol*. 2008;146:496–500.
6. Coscas F, Coscas G, Souied E, et al. Optical coherence tomography identification of occult choroid neovascularization in age-related macular degeneration. *Am J Ophthalmol*. 2007;144:592–599.
7. Spaide RF. Enhanced depth imaging optical coherence tomography of retinal pigment epithelial detachment in age-related macular degeneration. *Am J Ophthalmol*. 2009;147:644–652.
8. Podoleanu AG, Dobre GM, Cucu RC, et al. Combined multiplanar optical coherence tomography and confocal scanning ophthalmoscopy. *J Biomed Opt*. 2004;9:86–93.
9. Hee MR, Barnal CR, Puliafito CA, et al. Optical coherence tomography of age-related macular degeneration and choroidal neovascularization. *Ophthalmology*. 1996;103:1260–1270.
10. Blaauwgeers HG, Holtkamp GM, Rutten H, et al. Polarized vascular endothelial growth factor secretion by human retinal pigment epithelium and localization of vascular endothelial growth factor receptors on the inner choriocapillaris. Evidence for a trophic paracrine relation. *Am J Pathol*. 1999;155:421–428.
11. Kannan R, Zhang N, Sreekumar PG, et al. Stimulation of apical and basolateral VEGF-A and VEGF-C secretion by oxidative stress in polarized retinal pigment epithelial cells. *Mol Vis*. 2006;12:1649–1659.
12. Spilsbury K, Garrett KL, Shen WY, et al. Overexpression of vascular endothelial growth factor (VEGF) in the retinal pigment epithelium leads to the development of choroidal neovascularization. *Am J Pathol*. 2000;157:135–144.
13. Baffi J, Byrnes G, Chan CC, Csaky KG. Choroidal neovascularization in the rat induced by adenovirus mediated expression of vascular endothelial growth factor. *Invest Ophthalmol Vis Sci*. 2000;41:3582–3589.
14. Lumbroso B, Savastano MC, Rispoli M, Balestrazzi A, Savastano A, Balestrazzi E. Morphologic differences, according to etiology, in pigment epithelial detachments by means of en face optical coherence tomography. *Retina*. 2011;31:553–558.